

pubs.acs.org/est Article

# Effect of Nanoparticle Size and Natural Organic Matter Composition on the Bioavailability of Polyvinylpyrrolidone-Coated Platinum Nanoparticles to a Model Freshwater Invertebrate

Mithun Sikder, Marie-Noële Croteau, Brett A. Poulin, and Mohammed Baalousha\*



Cite This: https://dx.doi.org/10.1021/acs.est.0c05985



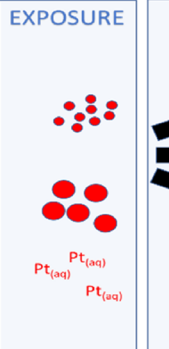
**ACCESS** 

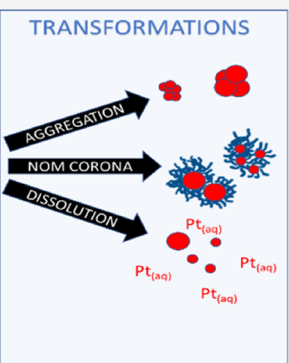
III Metrics & More



S Supporting Information

ABSTRACT: The bioavailability of dissolved Pt(IV) and polyvinylpyrrolidone-coated platinum nanoparticles (PtNPs) of five different nominal hydrodynamic diameters (20, 30, 50, 75, and 95 nm) was characterized in laboratory experiments using the model freshwater snail Lymnaea stagnalis. Dissolved Pt(IV) and all nanoparticle sizes were bioavailable to L. stagnalis. Platinum bioavailability, inferred from conditional uptake rate constants, was greater for nanoparticulate than dissolved forms and increased with increasing nanoparticle hydrodynamic diameter. The effect of natural organic matter (NOM) composition on PtNP bioavailability was evaluated using six NOM samples at two nanoparticle sizes (20 and 95 nm). NOM suppressed the bioavailability of 95 nm PtNPs in all cases, and DOM reduced sulfur content exhibited







a positive correlation with 95 nm PtNP bioavailability. The bioavailability of 20 nm PtNPs was only suppressed by NOM with a low reduced sulfur content. The physiological elimination of Pt accumulated after dissolved Pt(IV) exposure was slow and constant. In contrast, the elimination of Pt accumulated after PtNP exposures exhibited a triphasic pattern likely involving *in vivo* PtNP dissolution. This work highlights the importance of PtNP size and interfacial interactions with NOM on Pt bioavailability and suggests that *in vivo* PtNP transformations could yield unexpectedly higher adverse effects to organisms than dissolved exposure alone.

# INTRODUCTION

The bioaccumulation of engineered nanoparticles (NPs) depends largely on the exposed organisms, exposure conditions, and NP properties. Specifically, species-specific and metal-specific physiological processes (e.g., assimilation efficiencies and elimination rates 1-3), NP properties (e.g., size, 4 shape,<sup>5</sup> surface charge, surface coating, corona,<sup>6</sup> and concentration), physicochemical properties of the exposure media (e.g., ionic strength, pH, presence, and concentration of natural organic matter (NOM)),8 and NP behavior (e.g., aggregation, sedimentation, and dissolution)2 can affect the extent of NP bioaccumulation. However, these influences are equivocal. For example, studies have reported greater (e.g., AuNP<sup>4</sup> and AgNP<sup>9</sup>) and lower (e.g., AuNP, 10 AgNP, 11 ZnO-NP, 12 and SiO<sub>2</sub>-NP<sup>13</sup>) NP bioaccumulation with increasing NP size, as well as a lack of influence of NP (e.g., AuNP, 10 ZnO, TiO<sub>2</sub>, and SiO<sub>2</sub>-NP<sup>14</sup>) size on bioaccumulation. These discrepancies may be attributed to the NP size polydispersity, 15 NP aggregation and sedimentation in toxicological test media,<sup>2</sup> and differences among the in vivo models used by laboratories.

The influence of NOM on NP bioavailability and toxicity is multifaceted and understudied. Studies have shown that, for

the same type of NPs, NOM can enhance, 16 mitigate, 17,18 or exhibit no significant effects on NP bioavailability. 19 The variable impacts of NOM on NP bioavailability and toxicity may be due to differences in NOM molecular composition and, thus, NOM-NP surficial interactions (i.e., NOMcorona),8 which are not fully understood at the molecular level. Previous studies have used either model analogs for NOM (e.g., cysteine or citric acid)<sup>20</sup> or International Humic Substances Society NOM fractions (e.g., Suwannee River fulvic acid), 21 which do not accurately reflect the variability of NOM composition and properties in the environment. NOM is a complex mixture of polyelectrolytic and polyfunctional organic molecules<sup>22,23</sup> that vary spatially and temporally in terms of molecular composition, acidity, molecular weight, heteroatom composition, structure, and charge density.<sup>24</sup> The adsorption of NOM on NP surfaces results in the formation of NOM-

Received: September 4, 2020 Revised: January 19, 2021 Accepted: January 20, 2021



corona,<sup>25</sup> giving NPs a unique surface identity. NOM-corona can significantly impact the bioavailability and toxicity of NPs in aquatic organisms by altering NP fate and behavior.<sup>26</sup>

Bioaccumulation is often used as a proxy to bioavailability. Bioaccumulation represents the net outcome of both uptake and elimination processes.<sup>27</sup> For instance, high bioaccumulated metal concentrations can be achieved from fast metal uptake rates, slow elimination rates, or a combination of both processes. An improved understanding of the influence of NP size and NOM composition on NP bioavailability thus requires quantification of both uptake and elimination processes, which can help reconcile divergent results and better inform risk characterization.

Platinum group elements are increasingly released into the environment largely due to their use in automobile catalysts. Concentrations of Pt in the vicinity of roads have increased significantly in recent decades, reaching values of up to 50 ng kg<sup>-1</sup> in road dust,<sup>28</sup> 333  $\mu$ g kg<sup>-1</sup> in soil,<sup>29</sup> 10  $\mu$ g L<sup>-1</sup> in surface water,<sup>30</sup> 47  $\mu$ g kg<sup>-1</sup> in sediments,<sup>31</sup> and 12  $\mu$ g kg<sup>-1</sup> in plants.<sup>32</sup> The occurrence of PtNPs in the environment, notably in road dust,<sup>33</sup> raises concerns about their potential adverse environmental effects.<sup>34</sup> Bioaccumulation and toxicity have been reported in invertebrates,<sup>35</sup> microalgae,<sup>36</sup> and marine bacteria<sup>37</sup> exposed in the laboratory to Pt concentrations (e.g., 1-50 mg L<sup>-1</sup>) that often exceed most environmental exposures. In addition to lacking environmental relevance, these high exposure concentrations further influence NP aggregation and dissolution processes and, in the absence of NOM, confound conclusions of Pt bioavailability under conditions representative of the environment.<sup>38</sup>

This study quantified how Pt form (NP vs dissolved), PtNP size (20–95 nm), and NOM composition influence the bioavailability of Pt to a model aquatic invertebrate species. The importance of NOM composition on Pt bioavailability was assessed using six NOM isolates reflecting diverse source materials, properties, and aquatic environments. Using a bioaccumulation kinetic model,<sup>3</sup> we parameterized conditional rate constants for Pt uptake and elimination after short aqueous exposures to nanoparticulate Pt (five NP sizes) and dissolved Pt(IV) and qualified the importance of NP size and NOM properties. Findings from this study provide insights on the risk of metal-based nanoparticles in environmental systems.<sup>39,40</sup>

# MATERIALS AND METHODS

Nanoparticle Synthesis and Characterization. Polyvinylpyrrolidone-coated platinum engineered nanoparticles (PVP-PtNPs) were synthesized according to Sikder et al.<sup>41</sup> First, citrate-coated platinum engineered nanoparticles (cit-PtNPs) of different z-average hydrodynamic diameters (e.g., 10, 17, 31.6, 59.3, and 53.5 nm) were synthesized using a seedmediated growth approach as described elsewhere. 41 Second, PVP-PtNPs of different z-average hydrodynamic diameters designated as PtNP20, PtNP30, PtNP50, PtNP75, and PtNP95 were obtained by a ligand exchange approach using cit-PtNPs as precursors to obtain a surface coverage of eight PVP molecules per square nanometer. PVP-PtNPs were characterized using a suite of techniques including core diameter and morphology by transmission electron microscopy; elemental composition and purity by energy dispersive X-ray spectroscopy coupled with TEM; z-average hydrodynamic diameter (Z<sub>avg</sub>), polydispersity index (PDI), and electrophoretic mobility by dynamic light scattering (DLS) and laser Doppler

electrophoresis; and aggregation by monitoring the evolution of PtNP number size distribution and number and mass concentrations by single-particle inductively coupled plasma mass spectrometer (sp-ICP-MS) after (e.g., 0 and 24 h) mixing 1  $\mu$ g L<sup>-1</sup> PtNPs with moderately hard water (MHW).

Natural Organic Matter Samples. The hydrophobic acid (HPOA) fraction of NOM was isolated by the U.S. Geological Survey (USGS, George Aiken's laboratory)<sup>42</sup> from a wide range of aquatic environments including three saw-grass dominated wetlands in the northern Florida Everglades Water Conservation Area (WCA) 2A at site F1 (hereafter referred to as F1 HPOA), WCA 2B South (2BS HPOA), and Arthur R. Marshall Loxahatchee National Wildlife Refuge at site 8 (LOX8 HPOA); the Suwannee River (Georgia; SR HPOA); Williams Lake (Minnesota; WL HPOA); and Pacific Ocean surface water near Hawaii (PO HPOA). The HPOA fraction of NOM was isolated on XAD-8 resin, 43 which is a chemically distinct NOM fraction that is recognized as reactive to engineered NPs. 44 NOM samples were freeze-dried immediately after isolation to minimize NOM alteration prior to NP uptake experiments. Additional details on the isolation of the Everglades and Pacific Ocean samples are available elsewhere. 45,46 NOM samples were characterized for bulk elemental compositions (Huffman Hazen Laboratories, Golden, CO), specific ultraviolet absorbance at 254 nm (SUVA<sub>254</sub>) by UV-vis absorption spectroscopy,<sup>47</sup> molecular formulas and properties by Fourier transform ion cyclotron resonance mass spectroscopy (FT-ICR-MS),48 and sulfur speciation by sulfur K-edge X-ray absorption near-edge structure (XANES) spectroscopy as described in Poulin et al. (2017) (Tables S1 and S2 in the Supporting Information).<sup>45</sup> The concentration of reduced sulfur  $(S_{Red})$  in NOM is defined as the summation of exocyclic and heterocyclic reduced sulfur. 45,48

**Biodynamic Model.** A biodynamic model was used to quantify the mechanistic components of Pt bioaccumulation. The model accounts for Pt uptake, physiological elimination, and body growth dilution (detailed description is provided in the Supporting Information). Changes in Pt concentration in an organism ( $[Pt]_{org}$ ) over time after waterborne exposure are modeled as (eq 1):

$$\frac{[\text{Pt}]_{\text{org}}}{dt} = k_{\text{uw}} \times [\text{Pt}]_{\text{water}} - k_{\text{e}} \times [\text{Pt}]_{\text{org}} - k_{\text{g}} \times [\text{Pt}]_{\text{org}}$$
(1)

where  $k_{\rm uw}$  (L g<sup>-1</sup> d<sup>-1</sup>) is the unidirectional Pt influx rate constant from the solution, [Pt]<sub>water</sub> ( $\mu$ g L<sup>-1</sup>) is the aqueous total Pt concentration, and  $k_{\rm e}$  (d<sup>-1</sup>) and  $k_{\rm g}$  (d<sup>-1</sup>) are rate constants for physiological elimination and body growth dilution, respectively. Parameterization of the rate constants is described below and in the Supporting Information (eqs S2–S3).

**Experimental Organisms.** Freshwater snails (*Lymnaea stagnalis*) were reared in the laboratory in MHW (hardness around 80-100 mg of  $CaCO_3$  L<sup>-1</sup>, pH 8.1; Table S3 in the Supporting Information). Snails originated from a culture obtained 15 years ago from the University of Miami. They have been kept in 40 L glass tanks and fed lettuce weekly. Egg bags have been removed monthly when refreshing the media (MHW) and placed in a separate aquarium to form a new cohort every 3-4 months. Three days prior to each experiment, 70 juvenile snails of a restricted size range (average soft tissue dry weight of  $9.9 \pm 0.5$  mg, n = 344)

were transferred to a 10 L glass aquarium with freshly prepared MHW without food to depurate, thereby minimizing the production of feces during the subsequent exposures. Constraining the size of the experimental organisms allowed minimizing allometric effects on bioaccumulation. 50

**Waterborne Uptake Experiments.** The uptake of dissolved Pt(IV) (added as  $H_2PtCl_6$ ) and 19 nm PtNPs ( $PtNP_{20}$ ) in L. stagnalis was quantified after a short exposure (24 h) to five nominal Pt concentrations ranging from 0.01 to  $100~\mu g~L^{-1}$  in MHW (1 L), and a control with only MHW was included. Platinum concentrations span the expected range in aquatic environments.  $^{28}~k_{uw}$  specific to each Pt form (Pt(IV) and  $PtNP_{20}$ ) was determined from the slope of the linear relationship between Pt uptake rates and the exposure concentrations.

The effects of nanoparticle size and NOM composition on Pt uptake in L. stagnalis were characterized at one Pt concentration (1  $\mu$ g L<sup>-1</sup>) in MHW. By generating 5-times fewer samples than the parameterization described above, this approach allowed the screening of the effect of NP sizes and NOM isolates on Pt bioavailability. The  $k_{\rm uw}$  was determined by dividing the Pt uptake rate by the exposure concentration. Similarly, the effect of NOM on Pt bioavailability was evaluated by exposing snails to 1  $\mu$ g L<sup>-1</sup> of Pt(IV), PtNP<sub>20</sub>, or PtNP<sub>95</sub> in the presence of 1 mg L<sup>-1</sup> of each of the six NOM samples (Table S1). NOM-specific  $k_{\rm uw}$  values were determined as described for the size-specific  $k_{\rm uw}$  values.

All uptake experiments were performed in 1 L acid-washed high-density polyethylene (HDPE) containers using eight snails per exposure condition (experimental apparatus detailed in Table S4 in the Supporting Information). Food was not provided to minimize fecal scavenging.<sup>51</sup> The short exposure duration (24 h) minimizes the confounding influences of Pt elimination and fecal scavenging when parameterizing the unidirectional uptake rate constants for Pt from water ( $k_{uw}$ , eq 1). The exposures were of long enough duration, however, to ensure sufficient Pt accumulation for accurate detection. At the end of the exposure, snails were removed from the experimental media, rinsed with deionized water to remove surface-bound Pt or PtNPs, and frozen at −20 °C until analysis. Water samples were taken from each experimental container at the beginning (0 h, Pt<sub>0</sub>) and end of exposure (24 h) to determine Pt exposure concentrations (see section below) and evaluate particle dissolution by centrifugal ultrafiltration (see the Supporting Information).

Elimination Experiments. To characterize the physiological elimination of Pt accumulated after waterborne exposures, 65 snails were exposed to 10  $\mu$ g L<sup>-1</sup> dissolved Pt(IV), PtNP<sub>20</sub>, or PtNP<sub>95</sub> for 96 h. Snails were not fed during the exposure period to minimize fecal scavenging. After 96 h, snails were removed from the exposure media, rinsed thoroughly with MHW, and distributed into seven 150 mL acid-washed low-density polyethylene vials (each containing eight snails) that were partially submerged in a 40 L glass tank filled with 20 L of MHW (see Table S4). After 0, 1, 2, 3, 5, 7, and 10 days, snails were collected, rinsed with deionized water, and frozen at -20 °C until analysis. Aliquots of water (n = 3) were collected from the 40 L tank at each sampling time and acidified (1% volume to volume) with concentrated aqua regia. Snails were fed lettuce during the elimination period, and fecal material was removed from each chamber prior to adding fresh food and fully renewing the media every 2 days. Rate constants for physiological elimination  $(k_e, d^{-1})$  of Pt were quantified

based on the form of Pt (dissolved Pt(IV) vs PtNP) and size of PtNPs (PtNP<sub>20</sub> vs PtNP<sub>95</sub>) using a nonlinear regression model that includes compartments representing fast- and slow-exchanging pools (eq S2). Rate constants for body growth dilution ( $k_g$ ) were parameterized using an exponential growth curve (eq S3).

Sample Preparation for Pt Analysis. To minimize inadvertent metal contamination, laboratory ware, vials, and Teflon sheeting were soaked in 10% HNO<sub>3</sub> and/or 5% HCl for 24 h, then rinsed several times with ultrapure water (UPW, Milli-Q, 18 M $\Omega$ ), and dried under a laminar flow hood prior to use. Partially thawed L. stagnalis were dissected using fiber tip tweezers (Electron Microscopy). Soft tissues from each snail were dried (40 °C) for 3 days on acid-washed Teflon sheeting. Soft tissue dry weights were determined to the nearest microgram on a microbalance (Sartorius model M2P). Dry tissues were digested in polytetrafluoroethylene vials with 200 µL of aqua regia (freshly prepared from double-distilled HNO<sub>3</sub> and HCl) for 3 h at 125 °C in an autoclave (All American, model 50X). Digested samples were then diluted using ultrapure water (UPW, final volume 4 mL) and filtered (0.45 µm PVDF filter, Pall Corporation). An in-house reference tissue material was subjected to the same digestion procedure during each analytical run along with procedural blanks (see the Supporting Information). Water samples were acidified using 200 µL of freshly prepared aqua regia and diluted to 1% aqua regia.

All samples were analyzed for Pt by inductively coupled plasma mass spectroscopy (ICP-MS, PerkinElmer NexION 300Q). The ICP-MS was calibrated with 10, 100, 1000, and 10,000 ng L<sup>-1</sup> Pt standards. Thallium (Tl) was added to all samples, calibration standards, and blanks to monitor signal drift. One standard was also analyzed every 10 samples to monitor drift. Deviations from standard values were less than 10% for the analyzed Pt isotope ( $^{195}$ Pt). Recovery of the inhouse reference material was 95 ± 3%. Procedural blanks were below the method detection limit (MDL) for Pt of 0.005  $\mu$ g L<sup>-1</sup>. All data needed to evaluate the conclusions are presented in the paper, in the Supporting Information, and in Croteau et al. <sup>52</sup>

**Statistical Analysis.** Relationships between Pt influx rate constants and NOM elemental composition were evaluated using Pearson's correlations. Simple linear regression was used to quantify the relationships between Pt uptake rates and exposure concentrations for Pt(IV) and PtNP<sub>20</sub>. ANCOVA was used to determine if Pt bioavailability varied between Pt forms (Pt(IV) and PtNP<sub>20</sub>). Probability for the treatment by covariate interaction is reported. t tests were used to compare mean Pt influx rates between the control and a specific Pt exposure concentration. Data were examined for equality of variance and normality prior to assessing whether the Pt bioavailability and size of the experimental snails vary among treatments (PtNP sizes and NOM isolates) using either simple one-way ANOVA or Kruskal-Wallis, followed by pairwise multiple comparisons (Tukey test). Whether NP aggregate sizes varied in the presence or absence of NOM samples was similarly tested. In all cases, the statistical significance was set at p value < 0.05. Mean  $\pm$  standard deviation values are presented, unless otherwise mentioned.

# ■ RESULTS AND DISCUSSION

Particle Characterization and Behavior in Moderately Hard Water with NOM. The properties and behavior of

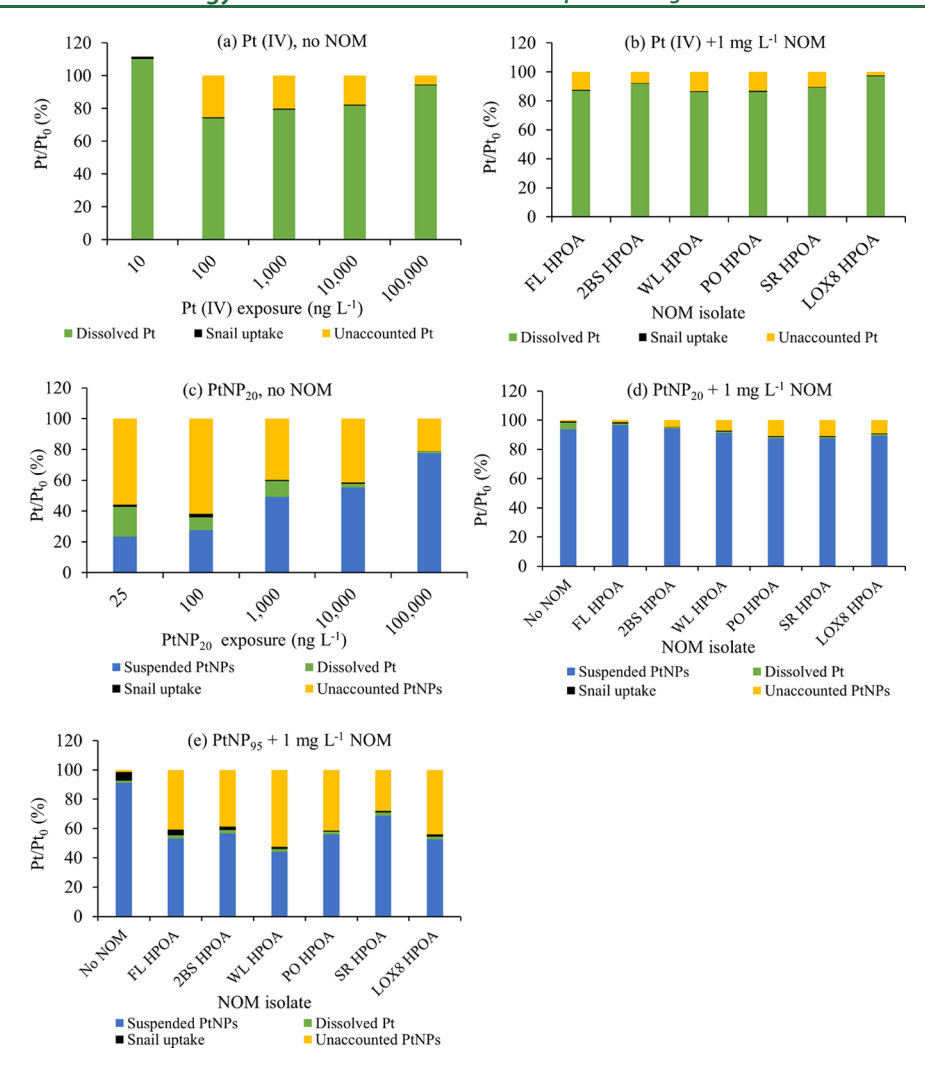


Figure 1. Distribution of Pt among the different phases after 24 h exposure for (a) different concentrations of dissolved Pt(IV) in the absence of natural organic matter (NOM), (b) 1  $\mu$ g L<sup>-1</sup> dissolved Pt(IV) in the presence of 1 mg L<sup>-1</sup> NOM isolates, (c) different concentrations of PtNP<sub>20</sub> in the absence of NOM, (d) 1  $\mu$ g L<sup>-1</sup> PtNP<sub>20</sub> in the presence of 1 mg L<sup>-1</sup> NOM isolates, and (e) 1  $\mu$ g L<sup>-1</sup> PtNP<sub>95</sub> in the presence of NOM 1 mg L<sup>-1</sup> NOM isolates. Calculations of Pt concentration in the different phases are provided in the Supporting Information.

PVP-PtNPs were determined using a multimethod approach as described and discussed in our previous studies. <sup>41</sup> Key data are briefly reported here. Core diameters (mean  $\pm$  standard deviation) of PtNP<sub>20</sub>, PtNP<sub>30</sub>, PtNP<sub>50</sub>, PtNP<sub>75</sub>, and PtNP<sub>95</sub> were  $9.2 \pm 1.2$ ,  $10.9 \pm 0.8$ ,  $18.5 \pm 5$ ,  $44.5 \pm 5$ , and  $72.5 \pm 3.9$  nm, respectively. The corresponding mean z-average hydrodynamic diameters were  $18.9 \pm 0.3$ ,  $31.4 \pm 0.8$ ,  $51 \pm 0.7$ ,  $74.7 \pm 0.2$ , and  $93.4 \pm 1$ , respectively. The zeta potential for the PtNPs decreased from  $-16.9 \pm 3.5$  to  $-27.2 \pm 1.7$  mV with increasing particle size (Table S5), reflecting the greater colloidal stability of the larger NPs.

All PtNPs (1  $\mu$ g L<sup>-1</sup>), except PtNP<sub>95</sub>, formed aggregates in MHW. PtNP<sub>20</sub> and PtNP<sub>30</sub> formed aggregates with smaller mean sizes (38  $\pm$  19 and 48  $\pm$  15 nm, respectively, measured by sp-ICP-MS) than PtNP<sub>50</sub> and PtNP<sub>75</sub> (54  $\pm$  10 and 62  $\pm$  9 nm, respectively, measured by sp-ICP-MS).<sup>48</sup> Nonetheless, suspensions of PtNP<sub>20</sub> and PtNP<sub>30</sub> formed aggregates with broader size distributions (*e.g.*, 15–100 and 15–100 nm, respectively) and contained larger aggregates than the suspension of PtNP<sub>75</sub> (*e.g.*, 15–75 nm). NP aggregate sizes were not significantly different in the presence or absence of NOM for both PtNP<sub>20</sub> and PtNP<sub>95</sub>, except in the presence of PO HPOA where PtNP<sub>20</sub> formed significantly larger aggregates

than those formed in the presence of all other NOMs and in the absence of NOM.  $^{48}$ 

Waterborne Pt Exposures. The Pt concentrations in the solution at different Pt(IV) exposure concentrations after 24 h of exposure in MHW (0.01-87.2  $\mu$ g L<sup>-1</sup>) represented 74  $\pm$  6 to  $110 \pm 5\%$  of the initial Pt concentrations (Pt<sub>0</sub>, 10-100,000ng L<sup>-1</sup>) (Figure 1a and Table S6a). The uptake of Pt(IV) by snails represented <2% of Pt<sub>0</sub>. The remaining fraction (<26% of  $Pt_0$  as Pt(IV) was likely removed from the solution through the binding of dissolved Pt species to snail exudates that settled out of the solution. The majority of dissolved Pt remained in the solution throughout the exposure experiments. In the presence of NOM, the dissolved Pt concentration after 24 h in MHW represented  $86 \pm 5$  to  $97 \pm 13\%$  of Pt<sub>0</sub> (Figure 1b and Table S6b). Uptake of Pt by snails represented <1% of Pt<sub>0</sub>. We attribute the remaining fraction (<14%) to the removal from the solution through the binding of dissolved Pt species to snail exudates.

The suspended PtNP<sub>20</sub> concentrations at different exposure concentrations after 24 h in MHW (0.007–69.9  $\mu$ g L<sup>-1</sup>) represented 23 ± 4 to 78 ± 4% of Pt<sub>0</sub> (Figure 1c and Table S7a). The dissolved Pt concentration measured after 24 h in MHW represented <10% of Pt<sub>0</sub>, except at the lowest exposure

concentrations. The Pt removed from the suspension after the uptake of PtNPs by snails represented <3% of Pt<sub>0</sub>. Between replicated exposures (1000 ng/L PtNP<sub>20</sub>), the proportion of Pt taken up by snails was identical (Table S7) despite differences in Pt partitioning (Figures 1c and 3). The remaining Pt fraction (<62% of Pt<sub>0</sub> as PtNP<sub>20</sub>) likely settled out of the suspension or stratified to lower depth in the water column (14 cm height) as the water samples were collected at 2.5 cm below the surface. According to Stokes's law, PtNP aggregates with sizes between 50 and 100 nm settle by 0.3 to 1.1 cm (Figure S1). These findings suggest that the majority of PtNPs, at these concentrations, were mostly insoluble and that significant sedimentation and/or stratification occurred during the exposures.

NOM did not affect the proportion of PtNP<sub>20</sub> in the suspension in the 1  $\mu$ g L<sup>-1</sup> exposure. The majority of PtNP<sub>20</sub> (88  $\pm$  7 to 97  $\pm$  4%) remained in the suspension in the presence and absence of NOM. Furthermore, PtNP<sub>20</sub> did not undergo substantial dissolution (<2%) or sedimentation ( $\leq$ 11%) (Figure 1d or Table S7b). The uptake of Pt by snails represented <1% of Pt<sub>0</sub>.

In the absence of NOM, PtNP<sub>95</sub> were stable with 91  $\pm$  14% of PtNPs remaining in the suspension, whereas  $1.5 \pm 0.3$ ,  $6 \pm$ 1, and 1.3  $\pm$  1% were accounted for by dissolution, uptake, and sedimentation, respectively. The addition of NOM destabilized PtNP<sub>95</sub> suspensions. The concentration of Pt remaining in the suspension after 24 h of PtNP<sub>95</sub> exposure in MHW in the presence of NOM represented 44  $\pm$  3 to 69  $\pm$  5% of the Pt<sub>0</sub> (Figure 1e and Table S7c). The dissolved Pt concentration after 24 h in MHW represented  $\leq$ 2% of Pt<sub>0</sub>. Pt uptake as PtNP<sub>95</sub> by L. stagnalis was greater than that for PtNP<sub>20</sub> but only accounted for <4% of Pt<sub>0</sub>. The remaining fraction of Pt  $(28-53\% \text{ of Pt}_0 \text{ as PtNP}_{95})$  likely settled out of the suspension. Using Stokes's law, we estimated that, in the absence of aggregation, PtNP<sub>95</sub> would have settled by approximately 1 cm in 24 h. PtNP<sub>95</sub> thus underwent substantial sedimentation in MHW in the presence of all NOM samples where aggregation was enhanced.

Pt Influx in L. stagnalis in the Absence of NOM. Pt influx in the snail soft tissues after exposures to dissolved Pt(IV) and PtNP<sub>20</sub> increased linearly with Pt concentrations ranging from 0.01 to 93  $\mu$ g L<sup>-1</sup> (p < 0.001, Figure 2). Pt concentration in control snails averaged  $3 \pm 1$  ng g<sup>-1</sup> (n = 8), which was similar to the Pt measured in snails exposed to the lowest Pt(IV) concentration (p = 0.05). Inadvertent minor contamination of the control solution likely explains the presence of Pt in the control snails (Table S7a), but this was inconsequential on the inference of bioavailability. Pt bioavailability varied between forms (p < 0.001). The Pt influx rate constants ( $k_{uw} \pm standard error in L g^{-1} d^{-1}$ ) were  $0.055 \pm 0.001$  for dissolved Pt(IV) and  $0.139 \pm 0.002$  for PtNP<sub>20</sub>, suggesting that Pt influxes are 2.5 times faster for the nanoparticulate than the dissolved Pt(IV) form. The effect of metal form (dissolved vs nanoparticulate) on uptake for Pt is opposite to that reported for Zn, Cu, and Ag, 53-56 which likely reflects the importance of nanoparticle uptake over the sole dependence to ion uptake, at least for the Pt NPs in these experimental conditions. The mechanistic reasons for this observation require further study. Differences among uptake rate constants from the solution also suggest a lower bioavailability for Pt to L. stagnalis than that observed for other metals under similar exposure routes and experimental conditions. For example, exposure to Ag from AgNO<sub>3</sub> or

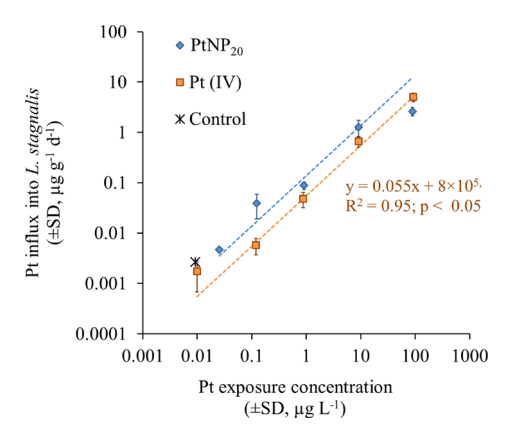


**Figure 2.** Platinum influx rates in *L. stagnalis* after waterborne exposure to Pt in the form of dissolved Pt(IV) (added as H<sub>2</sub>PtCl<sub>6</sub>) and 20 nm PVP-coated platinum nanoparticles (PtNP<sub>20</sub>). Each data point represents the mean Pt concentration for eight individual snails. The orange and blue dashed lines represent the linear relationship between Pt influx and the initial Pt exposure concentration. The star represents the Pt concentration in control snails.

citrate-capped AgNPs yielded  $k_{\rm uw}$  values of 1.1 and 0.35 L g<sup>-1</sup> d<sup>-1</sup>, respectively.<sup>51</sup> The proportion of dissolved Pt at the beginning of the exposure to PtNP<sub>20</sub> in MHW varied from 7 to 19% (control treatment excluded, not shown). Newly dissolved Pt from PtNP<sub>20</sub> had no detectable influence on  $k_{\rm uw}$  (see the Supporting Information for additional details). Overall, Pt accumulation after PtNP<sub>20</sub> exposure can be attributed to the bioaccumulation of PtNPs.

The NP size-specific Pt  $k_{\rm uw}$  ( $\pm$  standard error in L g<sup>-1</sup> d<sup>-1</sup>) for the nanoparticles ranged from 0.09  $\pm$  0.01 to 0.75  $\pm$  0.34 for the smallest- and largest-sized PtNPs, respectively (Figure 3). The  $k_{\rm uw}$  for the PtNP<sub>20</sub> (0.092 L g<sup>-1</sup> d<sup>-1</sup>) was slightly lower than that determined in the first series of experiments when snails were exposed to a range of Pt concentrations (0.14 L g<sup>-1</sup> d<sup>-1</sup>, open circle in Figure 3). The differences in the size of *L. stagnalis* might explain, in part, the differences in  $k_{\rm uw}$  in the above-mentioned experiments (Table S8). While the  $k_{\rm uw}$  values

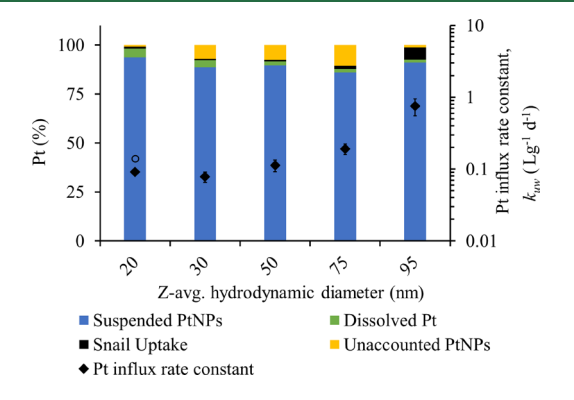
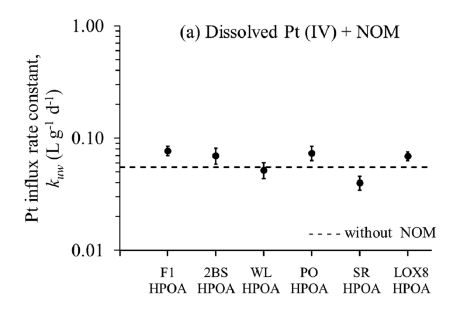


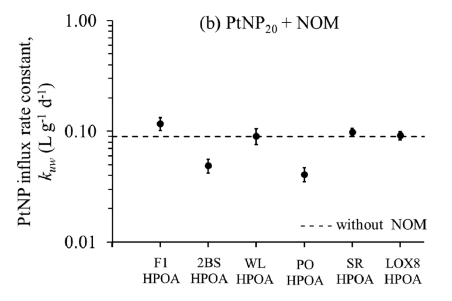
Figure 3. Platinum influx rate constant (black diamonds)  $k_{\rm uw}$  as a function of the z-average hydrodynamic diameter of PVP-PtNPs and distribution of Pt among the different phases following exposure to 1  $\mu \rm g \ L^{-1}$  PVP-PtNPs after 24 h (bars). The error surrounding the influx rate constant was determined by propagating the errors for the measured Pt influx in snail tissues and the corresponding Pt concentration in the media. The x-axis error bars are smaller than data points. The open circle represents  $k_{\rm uw}$  determined from the slope when NP $_{20}$  were exposed to L. stagnalis at five different concentrations (ranging from 0.01 to 100  $\mu \rm g \ L^{-1}$ ).

for PtNP<sub>20</sub>, PtNP<sub>30</sub>, and PtNP<sub>50</sub> were not significantly different (p > 0.9), the  $k_{uw}$  for PtNP<sub>95</sub> was significantly higher (p < 0.02)than the  $k_{uw}$  for all the other PtNPs tested (PtNP<sub>20</sub>, PtNP<sub>30</sub>, and PtNP<sub>50</sub>) except PtNP<sub>75</sub> (p > 0.7, Table S9). The  $k_{uw}$  for PtNP<sub>75</sub> was significantly higher than the  $k_{uw}$  values for the PtNP<sub>20</sub> and PtNP<sub>30</sub> (p < 0.05) but similar to that of PtNP<sub>50</sub> (p= 0.16) (Table S9). Because the size of the experimental snails was similar among treatments in these exposures (Table S8, p > 0.7), particle behavior(s) and/or characteristic(s) likely explain the increase in Pt bioavailability for the larger nanoparticle size. Sedimentation and/or stratification could not explain differences in PtNP bioavailability with nanoparticle size, as particle sedimentation and/or stratification only accounted for <1.2% of Pt<sub>0</sub> for the smallest and largest PtNP sizes (Table S7d and Figure 3). Therefore, the lower bioavailability of the smaller PtNPs might be attributed to particle aggregation as the smaller PtNPs (PtNP<sub>20</sub> and PTNP<sub>30</sub>) formed aggregates with broader size distributions containing larger and less bioavailable aggregates than the larger PtNPs (PtNP75 and PtNP90) that did not form aggregates.48

Effect of NOM Composition on Pt Influx. NOM did not influence the bioavailability of dissolved Pt(IV). The  $k_{max}$  values determined through the exposure of L. stagnalis to dissolved Pt(IV) in the presence of the six NOM samples were similar to the  $k_{\text{uw}}$  for dissolved Pt(IV) in the absence of NOM (Figure 4a). These results differ from the reported influence of NOM on waterborne metal bioavailability (i.e., Pb, Hg, Cd, Cu, Ag, U, and Co). 57-61 Aqueous metal speciation can considerably influence the bioavailability of metals.<sup>62</sup> However, little is known about the aqueous speciation of Pt in aquatic environments, especially in freshwaters and when NOM is present.<sup>63</sup> The outcomes of studies relating Pt bioavailability to aqueous speciation are equivocal. For instance, a greater uptake of Pt(IV) than Pt(II)64 has been reported for freshwater isopods, while a greater uptake of Pt(II) than Pt(IV) has been reported for zebra mussels.<sup>65</sup> Our results indicated that Pt(IV) is bioavailable in the dissolved phase to L. stagnalis, although bioavailability is less than that reported for other metals.

In contrast, NOM influenced the bioavailability of both the smallest and largest PtNPs tested. Specifically, Pt bioavailability from PtNP<sub>20</sub> exposure was suppressed in the presence of 2BS HPOA (45% suppression) and PO HPOA (55% suppression) compared to that in the absence of NOM (Figure 4b). Furthermore, all six NOM samples suppressed the bioavailability of PtNP<sub>95</sub> (Figure 4c). The extent of NOM suppression on Pt bioavailability from PtNP<sub>95</sub> exposures ranged from 39 to 90%. Differences in the size of the experimental organisms could not explain the differences in bioavailability (Table S8). The PtNP-specific and NOM-specific influences on Pt bioavailability can be attributed to (1) differences in the NOM molecular composition and properties, which may affect the properties of the PtNP NOM-corona, and/or (2) differences in the aggregation and sedimentation behaviors of the PtNPs (Figure 1d,e). For example, the suppression of Pt bioavailability for the PtNP<sub>20</sub> in the presence of 2BS HPOA and PO HPOA can be ascribed, in part, to the formation of larger PtNP<sub>20</sub> aggregates in the presence of these two NOM samples compared to the other NOM samples. 48 Aggregate sizes of PtNP<sub>20</sub> in the presence of 2BS HPOA and PO HPOA were  $66 \pm 21$  and  $74 \pm 34$  nm, respectively, in contrast to  $42 \pm$ 10 nm in the absence of NOM. Such aggregation did not lead





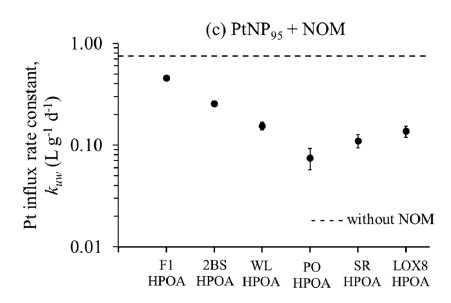


**Figure 4.** Platinum influx rate constant ( $k_{uw}$ ) in *L. stagnalis* after waterborne exposure to 1  $\mu$ g L<sup>-1</sup> of Pt in the form of (a) dissolved Pt(IV), (b) PtNP<sub>20</sub>, and (c) PtNP<sub>95</sub> for 24 h and distribution of Pt among the different phases. Dashed lines represent the Pt influx rate constant in the absence of NOM under the same exposure condition.

to substantial  $PtNP_{20}$  sedimentation and/or stratification (Figure 1d and Table S7b). Thus, differences in  $PtNP_{20}$  uptake in the presence of NOM might be attributed to differences in their aggregation behavior.

The sedimentation and/or stratification of Pt was 3–10 times greater for the PtNP<sub>95</sub> than the PtNP<sub>20</sub> in the presence of NOM (Figure 1d,e), which explains in part the overall lower bioavailability of the PtNP<sub>95</sub> in the presence of NOM (Figure 4c) compared to PtNP<sub>20</sub> in the presence of NOM (Figure 4b). Sedimentation and/or stratification does not fully explain the differences in the extent of bioavailability decrease in the presence of the different NOM samples. For instance, Pt bioavailability from PtNP<sub>95</sub> decreased following the order F1 HPOA >2BS HPOA > PO HPOA (Figure 4c), while the sedimentation (38.6  $\pm$  5 to 41.5  $\pm$  2.6) of PtNP<sub>95</sub> in the presence of these three NOMs was not significantly different (p > 0.1, Figure 1e).

Differences in NOM composition contributed to the observed differences in PtNP<sub>95</sub> bioavailability (Table S10). Pearson's correlation analyses between  $k_{\rm uw}$  of PtNP<sub>95</sub> and each NOM property revealed that the NOM sulfur content and speciation exhibited the best correlation coefficients (r=0.99, p<0.001) (Table S11), while weaker or lack of correlations was observed between  $k_{\rm uw}$  of PtNP<sub>95</sub> and NOM molecular weight; <sup>48</sup> SUVA<sub>254</sub>; and C, H, O, and N content (Figure S2

and Table S11). The reduced sulfur ( $S_{\rm red}$ ) content of the NOM samples, the summation of exocyclic and heterocyclic reduced sulfur, exhibited a strong positive correlation with  $k_{\rm uw}$  (p < 0.001, Table S11 and Figure 5). The stronger correlation

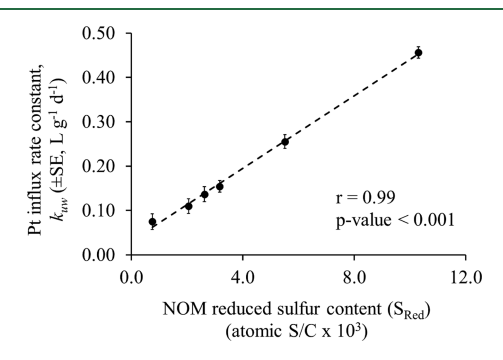


**Figure 5.** Correlation between the Pt influx rate constant  $(k_{uw})$  and NOM reduced sulfur concentration  $(S_{Red})$  following L. *stagnalis* exposure to  $1~\mu g~L^{-1}$  PtNP $_{95}$  in the presence of  $1~mg~L^{-1}$  NOM for 24 h. The black dashed lines represent the linear relationship between Pt influx rate and NOM  $S_{Red}$  content.

between  $k_{\rm uw}$  and the NOM reduced S content may be attributed to the higher affinity of reduced S for PtNP relative to oxidized S. All NOM samples suppressed the bioavailability of PtNP<sub>95</sub> compared to the NOM-free exposures. However, bioavailability was "less suppressed" for the NOM samples with more reduced S (Figure 4c). Mechanistic studies are needed to identify the reason for this finding, but we suspect that it is the result of interactions between the reduced S group in the NOM (e.g., thiols) and NP surfaces and/or newly dissolved Pt species (e.g., Pt(II)).

Physiological Loss of Accumulated Pt. The physiological elimination of Pt accumulated by L. stagnalis after aqueous exposure varied significantly between Pt forms (dissolved vs nanoparticulate). In addition to body growth dilution (Figure S4), Pt accumulated after exposure to dissolved Pt(IV) was steadily eliminated from the snail soft tissues (Figure 6a) with a rate constant of loss ( $k_e \pm 95\%$ confidence interval (CI)) of  $0.10 \pm 0.03 \text{ d}^{-1}$ , indicating that snails lost approximately 10% of their tissue burden of Pt per day through physiological elimination. L. stagnalis usually efficiently retained metal accumulated after dissolved exposures (i.e., Zn and Ag). 51,54 These results suggest a low retention of Pt accumulated after dissolved Pt exposures, which has been reported in a model mammalian species 40,75. In contrast to the steady elimination of Pt accumulated from dissolved Pt(IV) exposure, the loss of Pt accumulated after nanoparticle exposure followed a complex triphasic pattern. That is, 30 to 80% of the Pt accumulated after relatively short NP exposures was rapidly lost during the first 24 h of elimination (first phase; Figure 6b,c). This initial rapid loss is not unusual for metals and likely represents loss of loosely bound or surface-bound metals. 68,69 Longer metal exposures typically decrease the proportion of metals stored in this fast-exchanging compartment.<sup>70</sup> Elimination was not detected for the next 2-3 days (second phase). The transformation of the particles (e.g., dissolution) might have occurred during this phase, wherein tightly retained particles are transformed to ions that are more mobile. When loss resumed in the third phase, Pt from the smallest nanoparticles was steadily eliminated at a rate of 16% of the snail tissue burden of Pt per day. The loss of Pt from the largest PtNPs was faster  $(k_e \sim 1 \text{ d}^{-1})$ , but quantification was

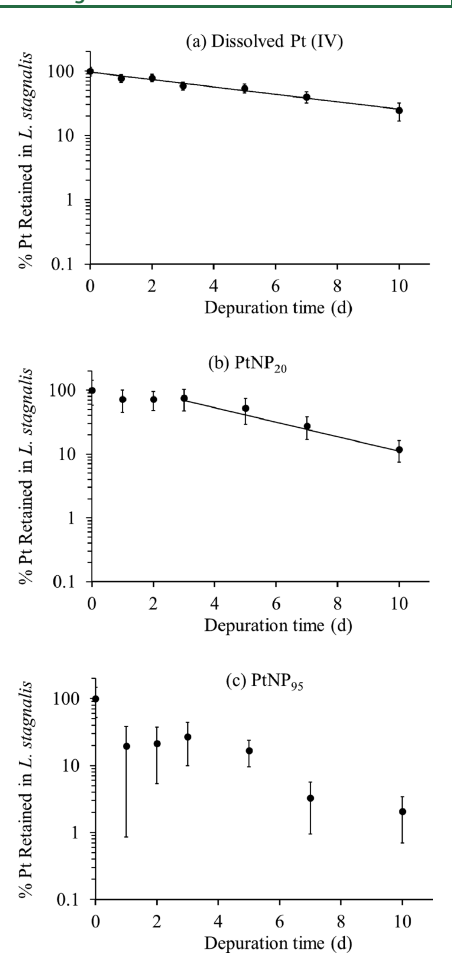


**Figure 6.** Proportional elimination of Pt from *L. stagnalis* after 24 h exposure to (a) dissolved Pt(IV), (b) PtNP<sub>20</sub>, and (c) PtNP<sub>95</sub>. Values represent the percentage (%) of Pt retained in *L. stagnalis* (mean  $\pm$  propagated error). Solid lines represent the loss modeled using a one-compartment model (plot a) and unidirectional loss from the second exchanging compartment (plot b).

less certain because the rate constant was estimated from only three data points (days 3, 5, and 7). These results suggest a unique pattern of loss for the studied Pt NPs. This triphasic pattern, unseen for dissolved metals, occurred with both Pt nanoparticle sizes. We interpret the continued loss of Pt in the third phase to the *in vivo* PtNP transformation and subsequent elimination of Pt. The similarity in  $k_{\rm e}$  values between dissolved Pt and PtNP<sub>20</sub> further suggests loss of dissolved Pt.

Overall, our results demonstrate that all forms of Pt (dissolved and nanoparticulate) are bioavailable to the model invertebrate L. stagnalis. PtNP size and NOM properties, in particular the NOM reduced S content, influence the bioavailability of PtNPs, especially for the larger-sized PtNPs. In the presence of NOM, bioavailability was reduced for the larger PtNPs (i.e., PtNP<sub>95</sub>) more than for the smaller PtNPs (i.e., PtNP<sub>20</sub>). This could be ascribed to the greater sedimentation and/or stratification of the larger nanoparticles (lower exposure concentrations from the suspended material rather than a difference in bioavailability). In the absence of NOM, the larger PtNPs are of greater bioavailability. The complex chemical reactivity of the smaller particles could explain this, the tendency of smaller aggregates to agglomerate into larger agglomerates. But in the presence of NOM, this effect is reversed, i.e., the larger particles are more affected and

larger agglomerates are formed. The potential for Pt bioaccumulation was estimated from the ratios between  $k_{\rm uw}$  and  $k_{\rm e}$  (from the slow-exchanging compartment) and increases in the order of Pt dissolved (0.60) < PtNP $_{20}$  (0.88) < PtNP $_{95}$  (1.0), suggesting that the influence of Pt form (dissolved Pt vs nanoparticulate) and PtNP size (larger vs smaller) on Pt bioaccumulation is modest, at least in this model species under the conditions tested. However, if nanoparticles are a vehicle to deliver more Pt into cells (e.g., Trojan horse $^{71}$ ), then it could result in unexpectedly higher adverse effects than dissolved Pt exposure alone. This effect will be of greater importance as exposure time increases (as is expected in nature) and more particles bioaccumulate into the slow-exchanging compartment of aquatic organisms.

# ASSOCIATED CONTENT

# **Solution** Supporting Information

The Supporting Information is available free of charge at https://pubs.acs.org/doi/10.1021/acs.est.0c05985.

Supplementary description and details on the isolation and characterization of natural organic matter (NOM) samples, biodynamic model, the chemical composition of the moderately hard water, assessment of the dissolution of PtNPs, and the preparation of platinum reference biological material. Figure S1 displays the sedimentation distance of PtNP aggregates as a function of aggregate size. Figure S2 illustrates the correlation between NOM properties and PtNP influx rate constant in *L. stagnalis* after exposure to 1  $\mu$ g L<sup>-1</sup> NP<sub>95</sub> in the presence of 1 mg L<sup>-1</sup> NOM for 24 h. Figure S3 illustrates the correlations between S species in NOM and Pt influx rate constant ( $k_{\rm uw}$ ) in  $\hat{L}$ . stagnalis after waterborne exposure to 1  $\mu {\rm g~L}^{-1}$  PtNP<sub>95</sub> in the presence of 1 mg L<sup>-1</sup> NOM for 24 h. Figure S4 illustrates the dry weight of snails during Pt elimination experiments following exposure to dissolved Pt, PtNP20, and PtNP<sub>95</sub>. Tables S1 and S2 provide the properties of the NOM samples. Table S3 presents the compostion of moderately hard water. Table S4 describes the experimental apparatus for the waterborne uptake and elimination experiments. Table S5 provides the zeta potential values of PtNPs of different sizes. Table S6 and S7 present the numerical values for the data presented in Figures 1 and 3. Table S8 illustrates the average dry weights of experimental snails for each experimental treatment. Table S9 summarizes the estimated values of biodynamic parameters used for or derived from modeling Pt accumulation and elimination in L. stagnalis. Table S10 summarizes the influx rate of PtNPs in the presence of NOM. Table S11 summarizes the Pearson's correlation coefficient between Pt influx rate constant and NOM properties for the PtNPos. (PDF)

# AUTHOR INFORMATION

# **Corresponding Author**

Mohammed Baalousha — South Carolina SmartState Center for Environmental Nanoscience and Risk (CENR), Department of Environmental Health Sciences, University of South Carolina, Columbia, South Carolina 29208, United States; orcid.org/0000-0001-7491-4954; Phone: +1 803-777-7177; Email: mbaalous@mailbox.sc.edu

## **Authors**

Mithun Sikder — South Carolina SmartState Center for Environmental Nanoscience and Risk (CENR), Department of Environmental Health Sciences, University of South Carolina, Columbia, South Carolina 29208, United States;
orcid.org/0000-0002-6295-0939

Marie-Noële Croteau — U.S. Geological Survey, Menlo Park, California 94025, United States; ⊙ orcid.org/0000-0003-0346-3580

Brett A. Poulin – U.S. Geological Survey, Boulder, CO 80303, United States; Department of Environmental Toxicology, University of California Davis, Davis, California 95616, United States; © orcid.org/0000-0002-5555-7733

Complete contact information is available at: https://pubs.acs.org/10.1021/acs.est.0c05985

#### Notes

The authors declare no competing financial interest.

### ACKNOWLEDGMENTS

This work was supported by US National Science Foundation NSF-EPSCoR Fellowship (1738340) to Dr. Mohammed Baalousha and by NSF to Dr. Brett Poulin (EAR-1629698). This research used resources of the Advanced Photon Source, a U.S. Department of Energy (DOE) Office of Science User Facility operated for the DOE Office of Science by Argonne National Laboratory under Contract No. DE-AC02-06CH11357. We are grateful to David Barasch for help with the snail culture and experimental approach, and Samuel Luoma for helpful comments on the manuscript. Any use of trade, firm, or product names is for descriptive purposes only and does not imply endorsement by the U.S. Government.

# REFERENCES

- (1) Lead, J. R.; Batley, G. E.; Alvarez, P. J. J.; Croteau, M. N.; Handy, R. D.; McLaughlin, M. J.; Judy, J. D.; Schirmer, K. Nanomaterials in the environment: Behavior, fate, bioavailability, and effects-An updated review. *Environ. Toxicol. Chem.* **2018**, *37*, 2029–2063.
- (2) Klaine, S. J.; Alvarez, P. J. J.; Batley, G. E.; Fernandes, T. F.; Handy, R. D.; Lyon, D. Y.; Mahendra, S.; McLaughlin, M. J.; Lead, J. R. Nanomaterials in the environment: Behavior, fate, bioavailability, and effects. *Environ. Toxicol. Chem.* **2008**, *27*, 1825–1851.
- (3) Luoma, S. N.; Rainbow, P. S. Why Is Metal Bioaccumulation So Variable? Biodynamics as a Unifying Concept. *Environ. Sci. Technol.* **2005**, *39*, 1921–1931.
- (4) Pan, J.-F.; Buffet, P.-E.; Poirier, L.; Amiard-Triquet, C.; Gilliland, D.; Joubert, Y.; Pilet, P.; Guibbolini, M.; de Faverney, C. R.; Roméo, M.; Valsami-Jones, E.; Mouneyrac, C. Size dependent bioaccumulation and ecotoxicity of gold nanoparticles in an endobenthic invertebrate: The Tellinid clam *Scrobicularia plana*. *Environ*. *Pollut*. **2012**, *168*, 37–43.
- (5) Ramskov, T.; Selck, H.; Banta, G.; Misra, S. K.; Berhanu, D.; Valsami-Jones, E.; Forbes, V. E. Bioaccumulation and effects of different-shaped copper oxide nanoparticles in the deposit-feeding snail *Potamopyrgus antipodarum*. *Environ*. *Toxicol*. *Chem.* **2014**, 33, 1976–1987.
- (6) Collin, B.; Oostveen, E.; Tsyusko, O. V.; Unrine, J. M. Influence of Natural Organic Matter and Surface Charge on the Toxicity and Bioaccumulation of Functionalized Ceria Nanoparticles in *Caenorhabditis elegans*. *Environ. Sci. Technol.* **2014**, 48, 1280–1289.
- (7) Sikder, M.; Eudy, E.; Chandler, G. T.; Baalousha, M. Comparative study of dissolved and nanoparticulate Ag effects on the life cycle of an estuarine meiobenthic copepod, *Amphiascus tenuiremis*. *Nanotoxicology* **2018**, *12*, 375–389.

- (8) Baalousha, M.; Afshinnia, K.; Guo, L. Natural organic matter composition determines the molecular nature of silver nanomaterial-NOM corona. *Environ. Sci.: Nano* **2018**, *5*, 868–881.
- (9) Lankveld, D. P. K.; Oomen, A. G.; Krystek, P.; Neigh, A.; Troost de Jong, A.; Noorlander, C. W.; Van Eijkeren, J. C. H.; Geertsma, R. E.; De Jong, W. H. The kinetics of the tissue distribution of silver nanoparticles of different sizes. *Biomaterials* **2010**, *31*, 8350–8361.
- (10) Skjolding, L. M.; Kern, K.; Hjorth, R.; Hartmann, N.; Overgaard, S.; Ma, G.; Veinot, J. G. C.; Baun, A. Uptake and depuration of gold nanoparticles in *Daphnia magna*. *Ecotoxicology* **2014**, 23, 1172–1183.
- (11) Zhao, C.-M.; Wang, W.-X. Size-Dependent Uptake of Silver Nanoparticles in *Daphnia magna*. *Environ. Sci. Technol.* **2012**, 46, 11345–11351.
- (12) Hao, L.; Chen, L.; Hao, J.; Zhong, N. Bioaccumulation and sub-acute toxicity of zinc oxide nanoparticles in juvenile carp (*Cyprinus carpio*): A comparative study with its bulk counterparts. *Ecotoxicol. Environ. Saf.* **2013**, *91*, 52–60.
- (13) Fujiwara, K.; Suematsu, H.; Kiyomiya, E.; Aoki, M.; Sato, M.; Moritoki, N. Size-dependent toxicity of silica nano-particles to Chlorella kessleri. J. Environ. Sci. Health, Part A 2008, 43, 1167–1173.
- (14) Adams, L. K.; Lyon, D. Y.; Alvarez, P. J. J. Comparative ecotoxicity of nanoscale TiO<sub>2</sub>, SiO<sub>2</sub>, and ZnO water suspensions. *Water Res.* **2006**, *40*, 3527–3532.
- (15) Baalousha, M.; Lead, J. R. Nanoparticle dispersity in toxicology. *Nat. Nanotechnol.* **2013**, *8*, 308.
- (16) Dasari, T. P.; Hwang, H.-M. The effect of humic acids on the cytotoxicity of silver nanoparticles to a natural aquatic bacterial assemblage. *Sci. Total Environ.* **2010**, 408, 5817–5823.
- (17) Fabrega, J.; Fawcett, S. R.; Renshaw, J. C.; Lead, J. R. Silver Nanoparticle Impact on Bacterial Growth: Effect of pH, Concentration, and Organic Matter. *Environ. Sci. Technol.* **2009**, 43, 7285–7290.
- (18) Wirth, S. M.; Lowry, G. V.; Tilton, R. D. Natural Organic Matter Alters Biofilm Tolerance to Silver Nanoparticles and Dissolved Silver. *Environ. Sci. Technol.* **2012**, *46*, 12687–12696.
- (19) Liu, X.; Jin, X.; Cao, B.; Tang, C. Y. Bactericidal activity of silver nanoparticles in environmentally relevant freshwater matrices: Influences of organic matter and chelating agent. *J. Environ. Chem. Eng.* **2014**, *2*, 525–531.
- (20) Luoma, S. N.; Stoiber, T.; Croteau, M.-N.; Römer, I.; Merrifeld, R.; Lead, J. R. Effect of cysteine and humic acids on bioavailability of Ag from Ag nanoparticles to a freshwater snail. *NanoImpact* **2016**, *2*, 61–69.
- (21) Wang, Z.; Zhang, L.; Zhao, J.; Xing, B. Environmental processes and toxicity of metallic nanoparticles in aquatic systems as affected by natural organic matter. *Environ. Sci.: Nano* **2016**, *3*, 240–255.
- (22) Keller, A. A.; Wang, H.; Zhou, D.; Lenihan, H. S.; Cherr, G.; Cardinale, B. J.; Miller, R.; Ji, Z. Stability and Aggregation of Metal Oxide Nanoparticles in Natural Aqueous Matrices. *Environ. Sci. Technol.* **2010**, *44*, 1962–1967.
- (23) Petosa, A. R.; Jaisi, D. P.; Quevedo, I. R.; Elimelech, M.; Tufenkji, N. Aggregation and Deposition of Engineered Nanomaterials in Aquatic Environments: Role of Physicochemical Interactions. *Environ. Sci. Technol.* **2010**, *44*, 6532–6549.
- (24) Gu, B.; Schmitt, J.; Chen, Z.; Liang, L.; McCarthy, J. F. Adsorption and desorption of different organic matter fractions on iron oxide. *Geochim. Cosmochim. Acta* 1995, 59, 219–229.
- (25) Lynch, I.; Dawson, K. A.; Lead, J. R.; Valsami-Jones, E. Macromolecular coronas and their importance in nanotoxicology and nanoecotoxicology. In *Frontiers of nanoscience*; Elsevier: 2014; 7, DOI: 10.1016/B978-0-08-099408-6.00004-9.
- (26) Praetorius, A.; Labille, J.; Scheringer, M.; Thill, A.; Hungerbühler, K.; Bottero, J.-Y. Heteroaggregation of Titanium Dioxide Nanoparticles with Model Natural Colloids under Environmentally Relevant Conditions. *Environ. Sci. Technol.* **2014**, *48*, 10690–10698.
- (27) Rainbow, P. S. Trace metal concentrations in aquatic invertebrates: why and so what? *Environ. Pollut.* **2002**, *120*, 497–507.

- (28) Ravindra, K.; Bencs, L.; Van Grieken, R. Platinum group elements in the environment and their health risk. *Sci. Total Environ.* **2004**, 318, 1–43.
- (29) Morton, O.; Puchelt, H.; Hernández, E.; Lounejeva, E. Trafficrelated platinum group elements (PGE) in soils from Mexico City. *J. Geochem. Explor.* **2001**, *72*, 223–227.
- (30) Zereini, F.; Skerstupp, B.; Alt, F.; Helmers, E.; Urban, H. Geochemical behaviour of platinum-group elements (PGE) in particulate emissions by automobile exhaust catalysts: experimental results and environmental investigations. *Sci. Total Environ.* **1997**, 206, 137–146.
- (31) de Vos, E.; Edwards, S. J.; McDonald, I.; Wray, D. S.; Carey, P. J. A baseline survey of the distribution and origin of platinum group elements in contemporary fluvial sediments of the Kentish Stour, England. *Appl. Geochem.* **2002**, *17*, 1115–1121.
- (32) Helmers, E. Platinum emission rate of automobiles with catalytic converters: Comparison and assessment of results from various approaches. *Environ. Sci. Pollut. Res.* **1997**, *4*, 99–103.
- (33) Folens, K.; Van Acker, T.; Bolea-Fernandez, E.; Cornelis, G.; Vanhaecke, F.; Du Laing, G.; Rauch, S. Identification of platinum nanoparticles in road dust leachate by single particle inductively coupled plasma-mass spectrometry. *Sci. Total Environ.* **2018**, *615*, 849–856.
- (34) Pawlak, J.; Łodyga-Chruścińska, E.; Chrustowicz, J. Fate of platinum metals in the environment. *J. Trace Elem. Med. Biol.* **2014**, 28, 247–254.
- (35) Veltz, I.; Arsac, F.; Biagianti-Risbourg, S.; Habets, F.; Lechenault, H.; Vernet, G. Effects of platinum (Pt<sup>4+</sup>) on Lumbriculus variegatus Muller (Annelida, Oligochaetae): acute toxicity and bioaccumulation. *Arch. Environ. Contam. Toxicol.* **1996**, *31*, 63–67.
- (36) Książyk, M.; Asztemborska, M.; Stęborowski, R.; Bystrzejewska-Piotrowska, G. Toxic Effect of Silver and Platinum Nanoparticles Toward the Freshwater Microalga *Pseudokirchneriella subcapitata*. Bull. Environ. Contam. Toxicol. **2015**, 94, 554–558.
- (37) Wei, C.; Morrison, G. M. Platinum in Road Dusts and Urban River Sediments. Sci. Total Environ. 1994, 146-147, 169-174.
- (38) Baalousha, M.; Sikder, M.; Prasad, A.; Lead, J.; Merrifield, R.; Chandler, G. T. The concentration-dependent behaviour of nanoparticles. *Environ. Chem.* **2016**, *13*, 1–3.
- (39) Wiesner, M. R.; Lowry, G. V.; Alvarez, P.; Dionysiou, D.; Biswas, P. Assessing the Risks of Manufactured Nanomaterials. *Environ. Sci. Technol.* **2006**, *40*, 4336–4345.
- (40) Colvin, V. L. The potential environmental impact of engineered nanomaterials. *Nat. Biotechnol.* **2003**, *21*, 1166–1170.
- (41) Sikder, M.; Wang, J.; Chandler, G. T.; Berti, D.; Baalousha, M. Synthesis, characterization, and environmental behaviors of monodispersed platinum nanoparticles. *J. Colloid Interface Sci.* **2019**, *540*, 330–341.
- (42) Chin, Y.-P.; McKnight, D.; Rosario-Ortiz, F. L. A Tribute to George R. Aiken. *Environ. Sci. Technol.* **2018**, *52*, 4489–4489.
- (43) Aiken, G. R.; McKnight, D. M.; Thorn, K. A.; Thurman, E. M. Isolation of hydrophilic organic acids from water using nonionic macroporous resins. *Org. Geochem.* **1992**, *18*, 567–573.
- (44) Jiang, C.; Castellon, B. T.; Matson, C. W.; Aiken, G. R.; Hsu-Kim, H. Relative Contributions of Copper Oxide Nanoparticles and Dissolved Copper to Cu Uptake Kinetics of Gulf Killifish (*Fundulus grandis*) Embryos. *Environ. Sci. Technol.* **2017**, *51*, 1395–1404.
- (45) Poulin, B. A.; Ryan, J. N.; Nagy, K. L.; Stubbins, A.; Dittmar, T.; Orem, W.; Krabbenhoft, D. P.; Aiken, G. R. Spatial Dependence of Reduced Sulfur in Everglades Dissolved Organic Matter Controlled by Sulfate Enrichment. *Environ. Sci. Technol.* **2017**, *51*, 3630–3639.
- (46) Green, N. W.; Perdue, E. M.; Aiken, G. R.; Butler, K. D.; Chen, H.; Dittmar, T.; Niggemann, J.; Stubbins, A. An intercomparison of three methods for the large-scale isolation of oceanic dissolved organic matter. *Mar. Chem.* **2014**, *161*, 14–19.
- (47) Weishaar, J. L.; Aiken, G. R.; Bergamaschi, B. A.; Fram, M. S.; Fujii, R.; Mopper, K. Evaluation of Specific Ultraviolet Absorbance as an Indicator of the Chemical Composition and Reactivity of

- Dissolved Organic Carbon. Environ. Sci. Technol. 2003, 37, 4702–4708.
- (48) Sikder, M.; Wang, J.; Poulin, B. A.; Tfaily, M. M.; Baalousha, M. Nanoparticle size and natural organic matter composition determine aggregation behavior of polyvinylpyrrolidone coated platinum nanoparticles. *Environ. Sci.: Nano* **2020**, *7*, 3318–3332.
- (49) US Environmental Protection Agency Methods for Measuring the Acute Toxicity of Effluents and Receiving Waters to Freshwater and Marine Organisms; U.S. EPA: Washington DC, 2002.
- (50) Stoiber, T.; Croteau, M. N.; Römer, I.; Tejamaya, M.; Lead, J. R.; Luoma, S. N. Influence of hardness on the bioavailability of silver to a freshwater snail after waterborne exposure to silver nitrate and silver nanoparticles. *Nanotoxicology* **2015**, *9*, 918–927.
- (51) Croteau, M.-N.; Misra, S. K.; Luoma, S. N.; Valsami-Jones, E. Silver Bioaccumulation Dynamics in a Freshwater Invertebrate after Aqueous and Dietary Exposures to Nanosized and Ionic Ag. *Environ. Sci. Technol.* **2011**, *45*, 6600–6607.
- (52) Croteau, M.-N.; Sikder, M.; Poulin, B. A.; Baalousha, M. Laboratory data to assess the effect of nanoparticle size and natural organic matter composition on the bioavailability of Pt nanoparticles to a model freshwater invertebrate species; U.S. Geological Survey: 2020; DOI: 10.5066/P9G18URX.
- (53) Zhao, C.-M.; Wang, W.-X. Biokinetic Uptake and Efflux of Silver Nanoparticles in *Daphnia magna. Environ. Sci. Technol.* **2010**, 44, 7699–7704.
- (54) Croteau, M.-N.; Dybowska, A. D.; Luoma, S. N.; Valsami-Jones, E. A novel approach reveals that zinc oxide nanoparticles are bioavailable and toxic after dietary exposures. *Nanotoxicology* **2011**, *5*, 79–90.
- (55) Croteau, M.-N.; Luoma, S. N.; Topping, B. R.; Lopez, C. B. Stable Metal Isotopes Reveal Copper Accumulation and Loss Dynamics in the Freshwater Bivalve Corbicula. Environ. Sci. Technol. **2004**, 38, 5002–5009.
- (56) Ramskov, T.; Croteau, M.-N.; Forbes, V. E.; Selck, H. Biokinetics of different-shaped copper oxide nanoparticles in the freshwater gastropod, *Potamopyrgus antipodarum*. Aquat. Toxicol. **2015**, 163, 71–80.
- (57) Trenfield, M. A.; Ng, J. C.; Noller, B. N.; Markich, S. J.; van Dam, R. A. Dissolved Organic Carbon Reduces Uranium Bioavailability and Toxicity. 2. Uranium[VI] Speciation and Toxicity to Three Tropical Freshwater Organisms. *Environ. Sci. Technol.* **2011**, 45, 3082–3089.
- (58) Gheorghiu, C.; Smith, D. S.; Al-Reasi, H. A.; McGeer, J. C.; Wilkie, M. P. Influence of natural organic matter (NOM) quality on Cu–gill binding in the rainbow trout (*Oncorhynchus mykiss*). *Aquat. Toxicol.* **2010**, *97*, 343–352.
- (59) Richards, J. G.; Curtis, P. J.; Burnison, B. K.; Playle, R. C. Effects of natural organic matter source on reducing metal toxicity to rainbow trout (*Oncorhynchus mykiss*) and on metal binding to their gills. *Environ. Toxicol. Chem.* **2001**, 20, 1159–1166.
- (60) Luider, C. D.; Crusius, J.; Playle, R. C.; Curtis, P. J. Influence of Natural Organic Matter Source on Copper Speciation As Demonstrated by Cu Binding to Fish Gills, by Ion Selective Electrode, and by DGT Gel Sampler. *Environ. Sci. Technol.* **2004**, *38*, 2865–2872.
- (61) De Schamphelaere, K. A. C.; Vasconcelos, F. M.; Tack, F. M. G.; Allen, H. E.; Janssen, C. R. Effect of dissolved organic matter source on acute copper toxicity to *Daphnia magna*. *Environ*. *Toxicol*. *Chem.* **2004**, 23, 1248–1255.
- (62) Campbell, P.; Ma, S.; Schmalzried, T.; Amstutz, H. C. Tissue digestion for wear debris particle isolation. *J. Biomed. Mater. Res.* **1994**, 28, 523–526.
- (63) Zimmermann, S.; Sures, B.; Ruchter, N. Laboratory Studies on the Uptake and Bioaccumulation of PGE by Aquatic Plants and Animals. In *Platinum Metals in the Environment*; Zereini, F., Wiseman, C. L. S., Eds.; Springer Berlin Heidelberg: Berlin, Heidelberg, 2015; pp. 361–381.
- (64) Rauch, S.; Morrison, G. M. Platinum uptake by the freshwater isopod *Asellus Aquaticus* in urban rivers. *Sci. Total Environ.* **1999**, 235, 261–268.

- (65) Zimmermann, S.; Alt, F.; Messerschmidt, J.; von Bohlen, A.; Taraschewski, H.; Sures, B. Biological availability of traffic-related platinum-group elements (palladium, platinum, and rhodium) and other metals to the zebra mussel (*Dreissena polymorpha*) in water containing road dust. *Environ. Toxicol. Chem.* **2002**, 21, 2713–2718.
- (66) Croteau, M. N.; Luoma, S. N. Characterizing dissolved Cu and Cd uptake in terms of the biotic ligand and biodynamics using enriched stable isotopes. *Environ. Sci. Technol.* **2007**, *41*, 3140–3145.
- (67) Croteau, M.-N.; Fuller, C. C.; Cain, D. J.; Campbell, K. M.; Aiken, G. Biogeochemical Controls of Uranium Bioavailability from the Dissolved Phase in Natural Freshwaters. *Environ. Sci. Technol.* **2016**, *50*, 8120–8127.
- (68) Cain, D.; Croteau, M.-N.; Luoma, S. Bioaccumulation dynamics and exposure routes of Cd and Cu among species of aquatic mayflies. *Environ. Toxicol. Chem.* **2011**, *30*, 2532–2541.
- (69) Henry, B. L.; Croteau, M.-N.; Walters, D. M.; Miller, J. L.; Cain, D. J.; Fuller, C. C. Uranium bioaccumulation dynamics in the mayfly *Neocloeon triangulifer* and application to site-specific prediction. *Environ. Sci. Technol.* **2020**, *54*, 11313–11321.
- (70) Riggs, D. S. The Mathematical Approach to Physiological Problems. *Acad. Med.* **1964**, *39*, 235.
- (71) Luoma, S. N. Silver nanotechnologies and the environment: Old problems or new challenges; Project on Emerging Nanotechnologies: Washington, DC, 2008.